# A Mixed-Integer-Linear-Logical Programming Interval-based Model for Optimal Scheduling of Isolated Microgrids with Green Hydrogen-based Storage considering Demand Response

Marcos Tostado-Véliz[1], Salah Kamel[2], Hany M. Hasanien[3], Rania A. Turky[4], Francisco Jurado[1,]*

[1]*Department of Electrical Engineering, University of Jaén, 23700 EPS Linares, Jaén, Spain*

[2]*Department of Electrical Engineering, Faculty of Engineering, Aswan University, Aswan 81542, Egypt*

[3]*Electrical Power and Machines Department, Faculty of Engineering, Ain Shams University, Cairo 11517, Egypt*

[4]*Electrical Engineering Department, Faculty of Engineering and Technology, Future University in Egypt, Cairo, Egypt*

*Abstract - Hydrogen produced from renewable sources (green hydrogen) will be recognized as one of the main trends in future decarbonized energy systems. Green hydrogen can be effectively stored from surplus renewable energy to thus reducing dependency of fossil fuels. As it is entirely produced from renewable sources, green hydrogen generation is strongly affected by intermittent behaviour of renewable generators. In this context, proper uncertain modelling becomes essential for adequately management of this energy carrier. This paper deals with this issue, more precisely, a novel optimal scheduling model for robust optimal scheduling of isolated microgrids is developed. The proposal encompasses a green hydrogen-based storage system and various demand-response programs. Logical rules are incorporated into the conventional optimal scheduling tool for modelling green hydrogen production, while uncertain character of weather and demand parameters is added via interval-based* *formulation and iterative solution procedure. The developed tool allows to perform the scheduling plan under pessimistic or optimistic point of views, depending on the influence assumed by uncertainties in the objective function. A case study serves to validate the model and highlight the paper of green hydrogen-based storage facilities in reducing fossil fuel consumptions and further exploit renewable sources.*

**Keywords:** Demand response, electrolyzer, fuel cell, green hydrogen, microgrid, renewable energy.

---------------------------------------------------------

*Corresponding author, Tel.: +34 953 648518; Fax: +34 953 648586.
E-mail addresses: fjurado@ujaen.es (F. Jurado), mtostado@ujaen.es (M. Tostado-Véliz), skamel@aswu.edu.eg (S. Kamel), hanyhasanien@ieee.org (H. M. Hasanien), Rania.turky@fue.edu.eg (R. A. Turky)

## Nomenclature

*Indexes(Sets)*

| | |
|---|---|
| $t(\mathcal{T})$ | Time |
| $s(\mathcal{S})$ | Sheddable consumer |
| $d(\mathcal{D})$ | Shiftable consumer |

*Superscripts*

| | |
|---|---|
| NS | Non-served |
| DEG | Diesel engine generator |
| PV | Photovoltaic |
| WG | Wind generation units |
| EZ | Electrolyser |
| FC | Fuel cell |
| LD | Local demand |
| HSS | Hydrogen storage system |
| $\overline{(*)}$/$\underline{(*)}$ | Maximum/minimum value |
| $\widehat{(*)}$ | Uncertain parameter |

*Parameters & constants*

| | |
|---|---|
| $\Delta\tau$ | Time step (h) |
| $\lambda$ | Penalization for loss load ($/kWh) |
| $\varrho$ | Penalization for shedding application ($/h) |
| $\upsilon$ | Penalization for unserved energy ($/kWh) |
| $\varepsilon$ | Total energy demanded by consumers subjected to shifting agreements (kWh) |
| $\omega_1^{DEG}$, $\omega_2^{DEG}$, $\omega_3^{DEG}$ | Cost coefficients of the DEG ($, $/kW, $/kW$^2$) |
| $\kappa$ | Capital cost ($/kW) |
| $\mu$ | Operation & maintenance cost ($/kWh) |
| $\nu$ | Start-up and shutdown costs ($) |
| $T$ | Number of life hours |
| $RD/RU$ | Ramping up/down rate limit (kW) |
| $\eta$ | Efficiency (p.u.) |
| $\alpha^{\mathrm{WG}}$,$\beta^{\mathrm{WG}}$ | Speed-power curve coefficients (kW·(m/s)$^{-3}$, -) |
| $\overline{v}^{\mathrm{HSS}}$ | Capacity of the hydrogen storage system (m$^3$) |
| $\theta^{\mathrm{HSS}}$ | Temperature inside the hydrogen tank (K) |
| LHV | Hydrogen lower heating value (J/mol) |
| $\mathfrak{R}$ | Gas constant (m$^3$·bar/(K·mol)) |
| $\xi$ | Uncertain level (-) |

*Interval modelling*

| | |
|---|---|
| $[a]$ | Uncertain parameter $a$ modelled as an interval number |
| $\mathbb{E}[a]$ | Expected value of the uncertain parameter $a$ |

*Decision variables*

| | |
|---|---|
| $p$ | Power (kW) |
| $n$ | Molar hydrogen (mol) |
| $g$ | Hydrogen pressure (bar) |

| | |
|---|---|
| $u$ | Commitment status (binary) |
| $\mathrm{on}_t^i/\mathrm{off}_t^i$ | Takes 1 if the unit $i$ is activated at time $t$, and 0 otherwise (binary) |

*Uncertain parameters ($\boldsymbol{\Omega}$)*

| | |
|---|---|
| $\theta^{\mathrm{air}}$ | Ambient temperature (ºC) |
| $\vartheta$ | Solar irradiance (kW/m$^2$) |
| $\gamma$ | Wind speed (m/s) |
| $d$ | Local non-sheddable/deferrable demand (kW) |

*Vectors notation*

| | |
|---|---|
| $\boldsymbol{w}$ | Vector of continuous variables |
| $\boldsymbol{u}$ | Vector of commitment (binary) variables |
| $\boldsymbol{\Omega}$ | Uncertain set |

# 1 - Introduction

## *1.1 - Context & motivation*

Hydrogen has gained an attention as future essential energy vector [1], especially the so-called green hydrogen, which is entirely produced through water electrolysis from renewable sources [2]. Different governmental entities and institutions are launching initiatives and projects to boost up investigation and use of this kind of source in future decarbonized energy systems [3]. Specifically, green hydrogen is expected to be one of the main energy sources in future smart cities [4]. Nowadays, European Union uses approximately 9.7 Mt of hydrogen annually, which needs to be decarbonized (i.e. converting it to green) [5].

Due to the increasing importance of green hydrogen in the upcoming energy sector, recent researches have been focused on improving the technology and efficiency of fuel cells (FCs) and electrolyzers (EZs) [6]. In this regard, reversible FCs have appeared as an attractive alternative to conventional devices, in order to improve the efficiency and economy of the hydrogen-based systems [7]. Emerging technologies such as solid-oxide FCs and EZs are gaining importance and are nowadays profusely studied for different applications, such as thermal energy storage by means of waste heat utilization [8] or co-electrolysis of water and CO2 [9]. Hydrogen can be stored in different states. The most conventional one is inside pressurized tanks [10], but emerging technologies such as metal hydride [11] and metal alloys [12] are being profusely studied to improve the efficiency, economy and security of the storage process.

In this context, it is observed a growing interest for integrating hydrogen generators and storage facilities with renewable sources such as photovoltaic (PV) and wind generation (WG) units, and demand-response (DR) programs [13]. To manage with intermittent nature and properly exploiting eventual surplus energy from renewable generators, hydrogen-based storage units which encompass EZs, hydrogen storage system (HSS) and FCs, become an essential facility to properly manage green hydrogen. More precisely, HSSs will play a vital role in energy management of isolated microgrids (MGs). Hydrogen-based storage has a higher energy density compared with traditional storage systems like Li-ion batteries [14]. Because this salient feature, HSSs are capable of storing large amounts of energy in a reduced space, thus supposing an attractive alternative to electro-chemical batteries. In this sense, hydrogen vessels may complement or even replace other technologies like batteries in MG applications [15].

*1.2 - Related works*

Some references have focused on energy market integration of HSSs, determining their optimal bidding strategy. In this regard, the reference [16] deals with the optimal integration of hydrogen-based systems in energy markets. To this end, a Mixed-Integer Linear programming (MILP) energy management problem is formulated, which determines the optimal bidding strategy in competitive electricity markets. On the other hand, the reference [17] also contemplates the implantation of price-based DR initiatives to improve the flexibility of the system. In both references, the uncertainties from renewable generation are modelled via stochastic programming. This approach requires to generate and solve a large amount of scenarios. In addition, a priori knowledge about probability distributions of uncertain parameters is needed. To circumvent such issues, the authors in [18] used information gap decision theory (IGDT) to model the uncertainties related with optimal bidding strategy of a hydrogen-based MG.

Other group of references is focused on the flexibility offered by smart parking lots. The model in [19] considers the response capability of vehicles charging processes, thus improving the economy of the retailer. The authors in [20] developed a multi-objective energy management problem, in which DR from charging infrastructures is considered and peak load management is incorporated as a secondary objective. Morzaghi, et al [21], developed an energy management model for smart parking lots integrated with HSSs. To manage with uncertainties from PV and WG, the authors employed interval arithmetic. The resulting bi-objective problem is then solved using the epsilon-constraint procedure. Similarly, interval arithmetic was considered in [22] to manage with uncertainties, employing in this case scalarizing functions to deal with the multi-objective optimization problem.

The reference [23] poses a multi-objective optimization approach for a hydrogen-based clean energy hub which considers economic, environmental and energy reserve objectives. In this model, DR is included by deferring the operation of EZs with hysteresis control under stochastic programming. In [24], the authors proposed a security constrained unit commitment for power systems with high penetration of wind energy, HSSs and DR programs. Kholardi, et al [25], proposed an energy hub model with consideration of the hydrogen network and thermal DR premises. The considered system comprises EZ, HSS and FC, and considers a bi-objective function with economic and environmental targets. The reference [26] deals with optimal sizing of HSSs for minimizing the intermittent impact of renewable generators. This model considers a flexible operation of hot water reservoirs.

The reference [27] proposed a three-level optimization framework, for optimal operation of an electric-hydrogen virtual power plant, which can sell/purchase energy in both electricity and hydrogen markets. Each level of the developed framework optimizes the energy flows in the system from different time scales. The article [28], deals with the optimal coordination of multiple Power-to-Hydrogen plants, with the objective of determining the most suitable hydrogen dynamic pricing and minimizing the joint operation cost. The different stations incorporate HSSs to participate in capacity ancillary services. In [29], the optimal operation of hydrogen-based storage system is performed through a bi-objective optimization procedure with scalarizing functions and max-min fuzzy decision-making technique.

The reference [30] deals with the optimal operation of a wind-based MG with HSSs. The optimization problem is solved via stochastic programming, incorporating risk-averse constraints and price-based DR programs. Mirzaei, et al [31], developed a stochastic security-constrained operation for a wind-HSS system in which a part of the demand is controllable under price-based DR programs. In [32], a stochastic-robust model for optimal coordination of WG units and HSS in a multi-energy hub is proposed, which aims at minimizing the total operational cost of the system. This reference contemplates price-based DR initiatives in both, electrical and thermal demand. The optimal operation of a multi-energy hub with power, gas, heating networks and HSS is addressed in [33], including the conditional value at risk in the model to count the uncertainty of wind speed. Shabani, et al, developed in [34] a decentralized framework for optimal coordination of various agents in a multi-energy system. The system comprises a HSS and DR in thermal, hydrogen and electrical loads.

The reference [35] addresses the optimal management of a multi-energy system with hybrid energy storage comprising HSS and batteries. In [36], a robust optimization approach is proposed for an energy hub which incorporates a storage system. The proposed model takes into account volatility of energy prices and contemplates possible revenues for selling hydrogen to a local consumer. Similarly, the reference [37] developed a hybrid robust-stochastic approach, by which the energy price is treated by robust optimization while remainder uncertainties are modelling via scenarios. Al Hajri, et al, developed in [38] a stochastic day-ahead unit commitment model for integrated electricity-gas networks. This model contemplates both HSS and plug-in electric vehicles, supplied by high penetration of renewable units.

### *1.3 - Contributions & paper organization*

Uncertainties modelling is one of the main concern when dealing with green hydrogen, due to stochastic essence of renewable generators. This aspect is especially relevant in isolated MGs, in which robust scheduling tools are essential for ensuring reliable supplying. In this regard, multiple approaches such as stochastic or robust programming, interval arithmetic or IGDT have been applied to HSSs. Table 1 summarizes the main features of the reviewed literature. On the basis of this analysis, the following research gaps have been encountered:

- Some references totally ignore the stochastic essence of renewable generation, while the majority of the literature employs stochastic-based approaches, which present a high computational burden and require a knowledge of the probability distributions of uncertain parameters.
- In most cases, only price-based DR programs are considered. This kind of initiatives find to shift the demand to off-peak periods through lower prices. However, further capabilities of DR schemes are seldom analyzed, such as the impact of incentive-based programs.

- Green hydrogen is normally not explicitly modelled. Instead, optimization problems assume that electrolyzers are only operated under eventual surplus renewable energy. However, this assumption does not ensure that produced hydrogen is totally green. This simplification may lead to generation of no-clean hydrogen, which may entail environmental concerns [2].

This paper is therefore motivated in the issues numerated above, and aims at solving them. To this end, a novel interval-based model for optimal scheduling of isolated MGs with green HSS and DR programs. In contrast to conventional interval-based formulations (e.g. see [21, 22]), the new proposal is inspired in [39], which takes advantage of the merits of conventional interval-based approaches but replacing the use of interval arithmetic by a simpler but reliable yet an iterative solution approach. This way, the MG operator can use forecast information of weather and demand forecast and their associated confidence intervals to carry out a robust scheduling plan of the MG. By this approach, it is avoided the resolution of a bi-objective optimization problem, as in the case of conventional interval-based approaches. Furthermore, the proposed approach allows to adopt optimistic or pessimistic strategies depending on the impact of uncertainties, which is not possible in other methodologies like stochastic programming. In addition, this paper presents the following relevant contributions:

- The developed optimization model incorporates detailed components modelling, which occasionally present nonlinearities. To preserve the linearity of the model, different linearization techniques are used and they are suitable to different nonlinearities encountered. This way, the resulting problem is a MILP, which is easily solvable by conventional software and present a modular structure [40], being so adaptable to different MG layouts.

- Mixed-Integer-Logical constraints are added to model green hydrogen production, so that the scheduling plan ensures that all the hydrogen produced in EZs is totally green.
- Different DR programs are considered. Thus, the studied MG incorporates various sheddable and deferrable consumers, which can be shut down or deferred if the scheduling plan thus considering. Establishing a series of penalty payments to compensate the application of DR premises.

As seen in Table 1, the new proposal supposes the first attempt to apply the iterative procedure in [39] to hydrogen-based MGs. In addition, the present research is, to the best of our knowledge, the first one to incorporate an explicit modelling of green hydrogen through logical constraints. A case study on a benchmark isolated MG is performed and various results are provided to validate the developed optimization model.

Table 1 - A summary of the literature review

| **Reference** | **Optimization model** | **Uncertainties modelling** | **DR** | **Green hydrogen modelling** |
|---|---|---|---|---|
| [16, 17] | MILP | Stochastic | Price-based | No |
| [18] | MILP | IGDT | Price-based | No |
| [19, 20, 30, 33, 34] | MILP | Stochastic | Price-based | No |
| [21, 22] | MILP | Interval arithmetic | Price-based | No |
| [23] | MILP | Stochastic | Incentive-based | No |
| [24-26, 29] | MILP | No | Price-based | No |
| [27] | Nonlinear | No | Price-based | No |
| [28] | Nonlinear | No | Incentive-based | No |
| [31, 38] | Nonlinear | Stochastic | Price-based | No |
| [32, 37] | MILP | Stochastic-robust | Price-based | No |
| [36] | MILP | Min-max | Price-based | No |
| Present | MILP | Forecast intervals (iterative) | Price-based Incentive-based | Logical constraints |

In the rest of this paper, Section 2 overviews the isolated system under study. Section 3 develops the mathematical models employed in the paper. The solution procedure for robust optimal scheduling of the MG under study using interval optimization is described in Section 4. Section 5 presents a case study and provides various numerical results. The paper is concluded with Section 6.

## 2 - Overview of the isolated system under study

This paper focuses on studying isolated MGs with green hydrogen-based storage system, which is schematically depicted in Fig. 1. The grid can supply the local demand by either renewable or backup generation through diesel engine generators (DEGs). Instead of conventional storage facilities formed by batteries, the studied MG incorporates a HSS with large storage capacity. As commented in the Introduction, reversible FCs could be used thus avoiding the necessity of EZs. Nevertheless, reversible FCs can be easily modelled as a FC + EZ system, in which each device simulates the charging/discharging processes of the HSS [41]. This is the reason why this paper assumes a conventional HSS formed by FC, pressurized hydrogen tank and EZ. The renewable generation is provided by PV and WG units. These generators can also produce hydrogen through water electrolysis. Hydrogen production is enabled when there is an excess of renewably energy, thereby, the hydrogen production is entirely green. The produced hydrogen is then stored in vessels, from which FCs can be supplied to generate electricity.

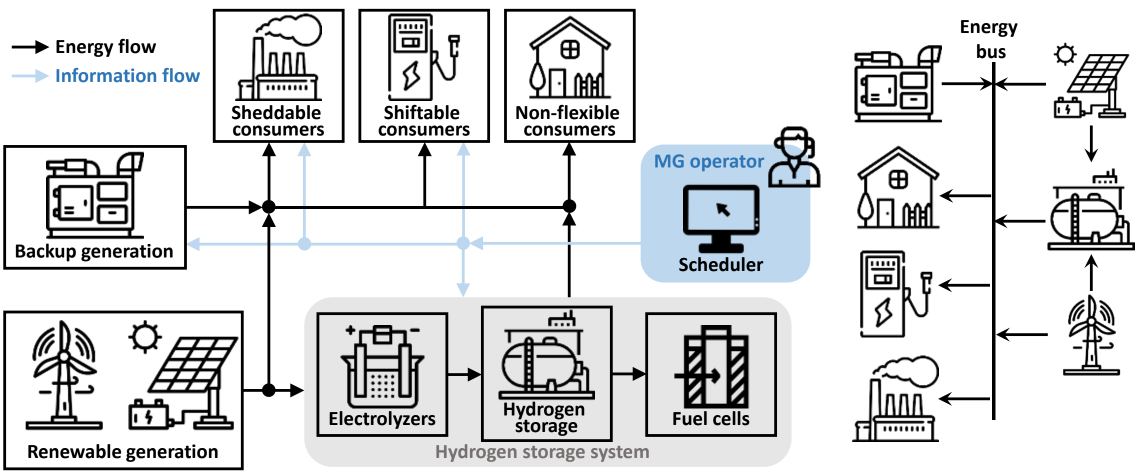


Figure 1 - Schematic representation (left) and single-line diagram (right) of the isolated system under study

The system under study contemplates various DR programs. On the other hand, a series of loads could be considered sheddable. These consumers may be directly disconnected from the grid, obtaining a compensatory payment for each hour that they are shut down [42]. This kind of DR is typical of large consumers, which may play a crucial role in power systems for ensuring the stability of the system. Nonetheless, in this paper their response might be still valuable for the MG operator, who could reduce the dependence of backup generators if penalization payments compensate the cost of diesel generation. In this sense, consumers agree a penalization payment which compensates the scheduled interruption of their consumption, which may presumably be deferred to other days. It is worth noting that interruption of sheddable loads is day-ahead scheduled, therefore, these consumers may properly adapt its routine according the programmed disconnections. Similarly, shiftable loads provide flexibility to the MG operation by deferring their consumption. Thus, these consumers agree an amount of energy that they desire to receive through the considered time horizon, however, this energy can be served whatever the scheduling plan determines most profitable. This kind of DR may be valuable for that kind of consumers which have certain storage capability, as for example electric vehicle recharging stations. Similar to sheddable consumers, the deferring loads obtain a monetary counterpart for each kWh that it is not served. The operator informs these consumers about the total quantity of energy that will be supplied, thus these consumers could schedule their internal operation accordingly. Finally, a large percentage of consumers is considered non-flexible and, therefore, their consumption patterns cannot be modified on the basis of price signals. Nevertheless, the MG can still decide no serving a percentage of the demand, paying a high penalization for each kWh non satisfied.

The MG operator daily performs a day-ahead scheduling plan for the MG under study. The scheduling tool consists on a robust optimization problem, that it is described in the following Section. For this task, operator requires forecast profiles for local demand and weather parameters. Conventional techniques normally provide confidence forecast intervals [43], within which the observed value may lie assuming a degree of probability. These intervals are essential for carrying out the developed scheduling problem, as explained in Section 3. With the necessary predicted information, the scheduling plan is calculated, which is transmitted to the different assets and consumers, as shown in Fig. 1. This operational principle is illustrated in Fig. 2. This paper does not deal with real time management, therefore, possible adjustments in the scheduling plan during the current day are not considered. For this task, a variety of real time management control are available in the literature (e.g. see [44]). Therefore, the developed tool is perfectly applicable to real cases, since the real-time control can be easily used in combination with the developed optimization model forming modular tools (e.g. see [45]). This feature is enabled because the MILP formulation of the developed day-ahead scheduling problem, since, as said in [40], this formulation presents a modular structure that allows it to be adapted to different cases and layouts.

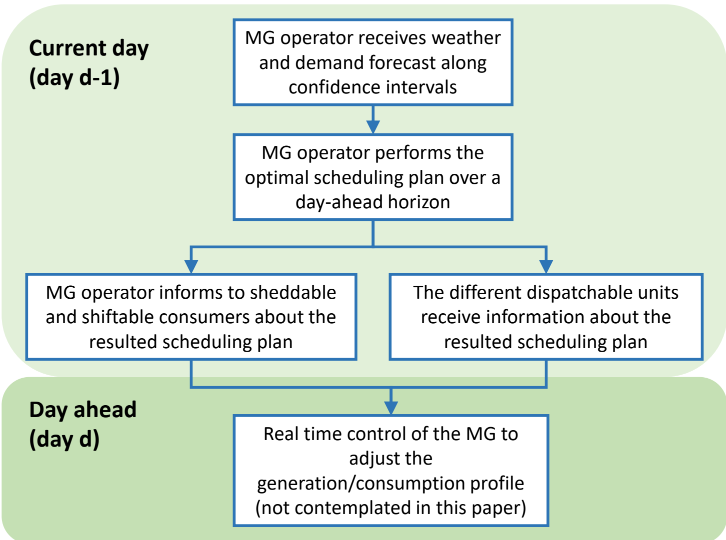


Figure 2 - Flowchart of the day-ahead scheduling procedure for the MG under study

## 3 - Mathematical models

This section describes the mathematical models for the optimal scheduling tool of the MG under study. For the formulation of the problem, a particular interval is utilized in formulation of uncertain parameters, which is firstly described.

### *3.1 - Interval numbers*

Interval arithmetic was firstly proposed by Moore [46] and has been extensively used in different problems [21, 22]. This approach represents an inexact parameter taking its expected value and maximum and minimum values, as follows:

$$[a] = \left[\bar{a}, \underline{a}\right] \tag{1a}$$
$$[a] = \left\{a \middle| \underline{a} \leq a \leq \bar{a}\right\} \tag{1b}$$

As commented, forecast techniques usually provide not only the expected value of a parameter, but also its confidence interval. In this paper, we propose an alternative formulation to (1), which fully exploits this information, as follows:

$$[a] = \langle \mathbb{E}[a], [a]^{\uparrow}, [a]^{\downarrow} \rangle \tag{2a}$$
$$\bar{a} = \mathbb{E}[a] + [a]^{\uparrow} \tag{2b}$$
$$\underline{a} = \mathbb{E}[a] - [a]^{\downarrow} \tag{2c}$$

As seen, by (2), the uncertain parameter $a$ is represented by its expected value and the amplitude of the predicted interval below and above the expected value. This approach is illustrated in Fig. 3.

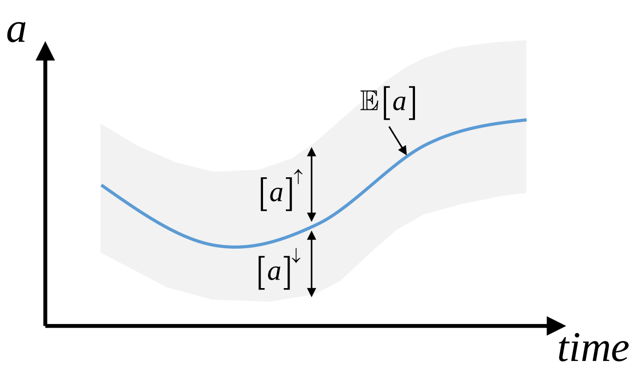


Figure 3 - Illustration of the interval approach used in this paper

*3.2 - MG energy balance*

The constraint in (3) ensures the generation-load balance in the MG any time instant. As seen, this expression includes the non-served load as an independent generator.

$$p_t^{\mathrm{DEG}} + p_t^{\mathrm{PV}} + p_t^{\mathrm{WG}} + p_t^{\mathrm{FC}} + p_t^{\mathrm{NS}} = [\hat{p}_t^{\mathrm{LD}}] + p_t^{\mathrm{EZ}} + \sum_{\forall s \in \mathcal{S}} \{u_t^s \cdot [\hat{p}_t^s]\} + \sum_{\forall d \in \mathcal{D}} \{p_t^d\};\ \forall t \in \mathcal{T} \quad (3)$$

*3.3 - Green hydrogen modelling*

As commented, the storage system contemplates in the MG depicted in figure 1 is based on green hydrogen production, therefore, all the hydrogen produced by electrolysis has to be generated from surplus renewable energy. In particular, surplus renewable energy in the case of the MG under study is given by:

$$\mathrm{SP}_t = \left[\hat{\phi}_t^{\mathrm{PV}}\right] + \left[\hat{\phi}_t^{\mathrm{WT}}\right] - \left[\hat{d}_t\right];\ \forall t \in \mathcal{T} \quad (4)$$

Equation (4) represents the net renewable potential at time $t$, which is positive if there is an excess of renewable generation and negative otherwise. To ensure that all the hydrogen produced is totally green, the following 'if' logical condition is imposed.

$$\begin{cases} p_t^{\mathrm{EZ}} \leq \mathrm{SP}_t, & \text{if } \mathrm{SP}_t > 0 \\ 0, & \text{o.w.} \end{cases};\ \forall t \in \mathcal{T} \quad (5)$$

By the constraint in (5), the total energy absorbed by the EZs is provided by renewable generators and, consequently, the hydrogen produced is green. The logical constraint in (5) can be converted to linear terms by using the big M method [47]. This approach requires to declare the dummy binary variable $\varpi^{(1)}$ and impose the following constraints.

$$M \cdot \varpi_t^{(1)} \geq \mathrm{SP}_t;\ \forall t \in \mathcal{T} \quad (6)$$

$$M \cdot \left(1 - \varpi_t^{(1)}\right) \geq -\mathrm{SP}_t;\ \forall t \in \mathcal{T} \quad (7)$$

where $M$ is a large positive number. It can be easily checked that $\varpi^{(1)} = 1$ if $\mathrm{SP}_t > 0$, and 0 otherwise. To complete the linear model of (5), it is necessary to impose the constraint in (8).

$$p_t^{\mathrm{EZ}} \leq \varpi_t^{(1)} \cdot \mathrm{SP}_t;\ \forall t \in \mathcal{T} \tag{8}$$

The constraint in (8) ensures that the total energy absorbed by the EZs does not surpass the total renewable surplus. When the interval numbers in (5) are declared as optimization variables (see Section 4), products of integer and continuous variables appear in (8). These terms can be easily linearized by declaring additional variables and constraints (see Appendix A).

*3.4 - Dispatchable units modelling*

In the MG described in Section 2, some units can be considered dispatchable. More specifically, DEG, EZ and FC can be scheduled on the basis of signals sent by the MG operator and determined by the scheduling tool. These units are normally described by lower and limit dispatchable powers and ramp constraints [48], as illustrated in (9) and (10), respectively. On the other hand, the equation (11) links the on/off and commitment variables.

$$u_t^i \cdot \underline{p}^i \leq p_t^i \leq u_t^i \cdot \overline{p}^i;\ \forall t \in \mathcal{T} \wedge i \in \{\mathrm{DEG}, \mathrm{EZ}, \mathrm{FC}\} \tag{9}$$

$$p_{t-1}^i - RD^i \leq p_t^i \leq p_{t-1}^i + RU^i;\ \forall t \in \mathcal{T} \backslash t > 1 \wedge i \in \{\mathrm{DEG}, \mathrm{EZ}, \mathrm{FC}\} \tag{10}$$

$$\mathrm{on}_t^i + \mathrm{off}_t^i = u_t^i - u_{t-1}^i;\ \forall t \in \mathcal{T} \backslash t > 1 \wedge i \in \{\mathrm{DEG}, \mathrm{EZ}, \mathrm{FC}\} \tag{11}$$

*3.5 - PV generators modelling*

PV potential generation is determined by weather parameters, more precisely, the maximum power that a PV generator can deliver is a function of the solar irradiation and ambient temperature, and can be calculated, as follows [49]:

$$\left[\hat{\phi}_t^{\mathrm{PV}}\right] = \overline{p}^{\mathrm{PV}} \cdot \left[0.25 \cdot \left[\vartheta_t\right] + 0.03 \cdot \left[\hat{\vartheta}_t\right] \cdot \left[\hat{\theta}_t^{\mathrm{air}}\right] + \left(1.01 - 1.13 \cdot \eta^{\mathrm{PV}}\right) \cdot \left[\hat{\vartheta}_t\right]^2\right];\ \forall t \in \mathcal{T} \tag{12}$$

As commented in [50], the expression above cannot be directly applied since its value can be occasionally higher than the installed peak power. To avoid this conflict, the following logical constraint can be imposed.

$$0 \leq p_t^{\mathrm{PV}} \leq \begin{cases} [\hat{\phi}_t^{\mathrm{PV}}], \text{if } [\hat{\phi}_t^{\mathrm{PV}}] \leq 1.1 \cdot \overline{p}^{\mathrm{PV}} \\ 1.1 \cdot \overline{p}^{\mathrm{PV}}, \qquad\qquad \text{o.w.} \end{cases}; \ \forall t \in \mathcal{T} \tag{13}$$

By the constraint in (13), the power given by PV units is limited to 10% over the installed peak power, which is a usual bound for PV installations [50]. When the interval numbers are declared optimization variables, the condition (13) can be linearized by using the big M method in a similar way to (5), as follows:

$$M \cdot \varpi_t^{(2)} \geq 1.1 \cdot \overline{p}^{\mathrm{PV}} - [\hat{\phi}_t^{\mathrm{PV}}]; \ \forall t \in \mathcal{T} \tag{14}$$

$$M \cdot \left(1 - \varpi_t^{(1)}\right) \geq [\hat{\phi}_t^{\mathrm{PV}}] - 1.1 \cdot \overline{p}^{\mathrm{PV}}; \ \forall t \in \mathcal{T} \tag{15}$$

$$p_t^{\mathrm{PV}} \leq \varpi_t^{(2)} \cdot [\hat{\phi}_t^{\mathrm{PV}}] + \left(1 - \varpi_t^{(2)}\right) \cdot \left(1.1 \cdot \overline{p}^{\mathrm{PV}}\right); \ \forall t \in \mathcal{T} \tag{16}$$

where $\varpi^{(2)}$ is analogue to $\varpi^{(1)}$ in (6)-(8). A product of the dummy integer variable $\varpi^{(2)}$ and the continuous one $[\hat{\phi}_t^{\mathrm{PV}}]$ appears in (16), which can be linearized following the procedure described in Appendix A. In the expression (12), a quadratic term due appears when solar irradiance is declared as a variable. To linearize this term, the procedure described in Appendix B can be used. Similarly, a bi-linear term may appear in (12) because the product of the solar irradiance and ambient temperature. This product can be linearized using advanced piecewise strategies (see Appendix C).

*3.6 - WG units modelling*

The power given by WG units is a function of the wind speed and is normally given by the well-known speed-power curves of the wind turbines [48], as shown in Fig. 4. As seen in this figure, these profiles are divided into 4 sections limited by characteristics wind speeds. These curves are normally facilitated by manufacturers and can be mathematically expressed as follows [48]:

$$[\hat{\phi}_t^{\mathrm{WG}}] = \begin{cases} 0, & \text{if } [\hat{\gamma}_t] < \underline{\gamma}^{\mathrm{WG}} \\ \alpha^{\mathrm{WG}} \cdot ([\hat{\gamma}_t])^3 - \beta^{\mathrm{WG}} \cdot \overline{p}^{\mathrm{WG}}, & \text{if } \underline{\gamma}^{\mathrm{WG}} \leq [\hat{\gamma}_t] \leq \gamma^{\mathrm{WG},*} \\ \overline{p}^{\mathrm{WG}}, & \text{if } \gamma^{\mathrm{WG},*} < [\hat{\gamma}_t] \leq \overline{\gamma}^{\mathrm{WG}} \\ 0, & \text{if } [\hat{\gamma}_t] > \overline{\gamma}^{\mathrm{WG}} \end{cases}; \ \forall t \in \mathcal{T} \tag{17}$$

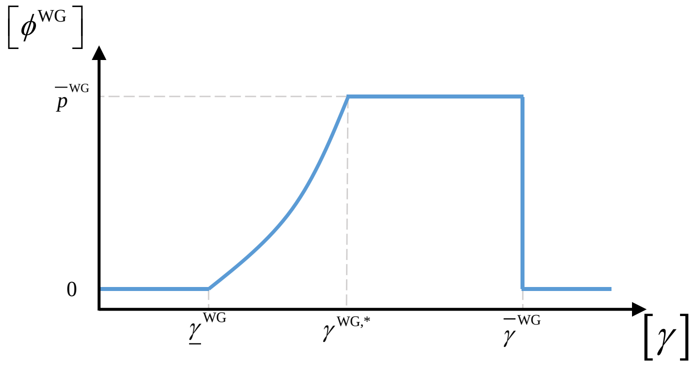


Figure 4 - Typical speed-power curve of a wind turbine

To linearize the model (17), a piece representation of the speed-power curve into 5 sections is proposed as follows:

$$\tilde{\psi} = \left\{ \langle \tilde{\gamma}_i \rangle \;\middle|\; \begin{array}{l} \tilde{\gamma}_1 = 0 \\ \tilde{\gamma}_2 = \underline{\gamma}^{\mathrm{WG}} \\ \tilde{\gamma}_3 = \gamma^{\mathrm{WG},*} \\ \tilde{\gamma}_4 = \overline{\gamma}^{\mathrm{WG}} \\ \tilde{\gamma}_5 = M \end{array} \right. \quad (18)$$

The piece representation in (18) can be efficiently linearized by introducing the integer set $\varsigma$, which has 4 dimensions, and imposing the constraints (19) and (20).

$$\sum_{i=1}^{i=4}\{\varsigma_{i|t} \cdot \tilde{\gamma}_i\} \leq [\hat{\gamma}_t] \leq \sum_{i=2}^{i=5}\{\varsigma_{i-1|t} \cdot \tilde{\gamma}_i\};\ \forall t \in \mathcal{T} \quad (19)$$

$$p_t^{\mathrm{WG}} = \varsigma_{1|t} \cdot 0 + \varsigma_{2|t} \cdot \left(\alpha^{\mathrm{WG}} \cdot [\hat{\gamma}_t]^3 - \beta^{\mathrm{WG}} \cdot \overline{p}^{\mathrm{WG}}\right) + \varsigma_{3|t} \cdot \overline{p}^{\mathrm{WG}} + \varsigma_{4|t} \cdot 0;\ \forall t \in \mathcal{T} \quad (20)$$

The equation (19) determines which element of the set $\varsigma$ according the wind speed any moment, while the model (20) yields the power given by WG units using the piece model (18). To ensure that only one element of the set $\varsigma$ is activated at once, it can be declared a special ordered set 1 (see [51]). On the other hand, the cubic term in (20) can be linearized using piecewise representations (see Appendix B) while the product of integer and continuous variables are linearized following the model described in Appendix A. The wind turbine model is completed by introducing the efficiency, as said the equation (21).

$$0 \leq p_t^{\mathrm{WG}} \leq \eta^{\mathrm{WG}} \cdot [\hat{\phi}_t^{\mathrm{WG}}];\ \forall t \in \mathcal{T} \quad (21)$$

*3.7 - Hydrogen storage modelling*

The set of constraints (22)-(27) model the HSS contemplated in the MG under study, and corresponds with modified versions of other standard modelling (e.g. see [19, 52]).

$$n_t^{\mathrm{EZ}} = \frac{\eta^{\mathrm{EZ}} \cdot p_t^{\mathrm{EZ}}}{\mathrm{LHV}}; \ \forall t \in \mathcal{T} \tag{22}$$

$$n_t^{\mathrm{FC}} = \frac{p_t^{\mathrm{FC}}}{\eta^{\mathrm{FC}} \cdot \mathrm{LHV}}; \ \forall t \in \mathcal{T} \tag{23}$$

$$g_t^{\mathrm{HSS}} = g_{t-1}^{\mathrm{HSS}} + \frac{\theta^{\mathrm{HSS}} \cdot \mathfrak{R}}{\overline{v}^{\mathrm{HSS}}} \cdot \left(n_t^{\mathrm{EZ}} - n_t^{\mathrm{FC}}\right); \ \forall t \in \mathcal{T} \backslash t > 1 \tag{24}$$

$$\underline{g}^{\mathrm{HSS}} \leq g_t^{\mathrm{HSS}} \leq \overline{g}^{\mathrm{HSS}}; \ \forall t \in \mathcal{T} \tag{25}$$

$$\textstyle\sum_{\forall i \in \{\mathrm{EZ},\mathrm{FC}\}} \left\{u_t^i\right\} \leq 1; \ \forall t \in \mathcal{T} \tag{26}$$

The equations (22) and (23) are the molar hydrogen production/absorption, as function of the electrical power absorbed/generated by EZ/FC. The equation (24) models the state of pressure inside the hydrogen tank, which must lie within acceptable limits, as said the constraint (25), whereas the constraint in (26) avoids the simultaneous charging-discharging of the hydrogen tank. Similar to conventional models used for batteries (e.g. see [48]), the initial pressure of the hydrogen tank must be set since the equation (24) is not defined for $t = 1$. In this work, as customary for other storage technologies, it is assumed that the hydrogen tanks are totally filled at the beginning of the time horizon. In order to keep the model coherent, the constraint (27) ensures that the final status of the HSS is equal to the initial state of charge.

$$g_{t=1}^{\mathrm{HSS}} = g_{t=\mathrm{end}}^{\mathrm{HSS}} = \overline{g}^{\mathrm{HSS}} \tag{27}$$

*3.8 - Shiftable consumers modelling*

It is realistic to assume that power supplied to shiftable consumers should be limited by any type or physical or contractual bound, as said the constraint (28). On the other hand, the constraint in (29) is included to avoid incoherency in the objective function.

$$0 \leq p_t^d \leq \overline{p}^d; \ \forall t \in \mathcal{T} \wedge d \in \mathcal{D} \tag{28}$$

$$\textstyle\sum_{\forall t \in \mathcal{T}} \{p_t^d\} \leq \varepsilon^d; \ \forall t \in \mathcal{T} \wedge d \in \mathcal{D} \tag{29}$$

*3.9 - Objective function*

The MG operator presumably aims at minimizing the total operating cost of the system. According to the description in Section 2, the operating cost of the MG under study encompasses various terms, as follows:

$$f = f^{\mathrm{Shedding}} + f^{\mathrm{Shifting}} + f^{\mathrm{NS}} + f^{\mathrm{DEG}} + f^{\mathrm{PV}} + f^{\mathrm{WT}} + f^{\mathrm{EZ}} + f^{\mathrm{FC}} \tag{30}$$

It is noteworthy that despite the objective function (30) involves eight terms, all of them are referred to different costs which, in combination, yield the total daily operational cost of the MG under study. Therefore, due to all of terms in (30) are referred to monetary units, the resulting optimization problem is solved as a single-objective approach since the unique target is the minimization of the total expenditures.

The first two terms in (30) are the cost of penalizations due to application of DR programs. For the sheddable consumers, these payments are proportional to the total number of hours that they are forced to be disconnected from the grid, and can be calculated as follows:

$$f^{\mathrm{Shedding}} = \sum_{\forall s \in \mathcal{S}} \{\Delta\tau \cdot \varrho^{s} \cdot (\mathcal{T} - \sum_{\forall t \in \mathcal{T}} \{u_t^s\})\} \tag{31}$$

For the shiftable consumers, penalizations are established proportional to the deviation of the amount of energy agreed with the operator. Therefore, the total penalty cost in which the system incurs for shiftable demands is given by:

$$f^{\mathrm{Shifting}} = \sum_{\forall d \in \mathcal{D}} \left\{\upsilon^{d} \cdot \left(\varepsilon^{d} - \Delta\tau \cdot \sum_{\forall t \in \mathcal{T}} \{p_t^d\}\right)\right\} \tag{32}$$

The third term in (30) is the cost of non-served energy. In this paper, non-served load is treated as an independent generator with its own associated cost per kWh. This way, the cost of non-served load can be easily calculated by (33), while (34) establishes coherent limits for the variable.

$$f^{\mathrm{NS}} = \sum_{\forall t \in \mathcal{T}} \left\{\Delta\tau \cdot \lambda^{\mathrm{NS}} \cdot p_t^{\mathrm{NS}}\right\} \tag{33}$$

$$0 \le p_t^{\mathrm{NS}} \le [\hat{p}_t^{\mathrm{LD}}];\ \forall t \in \mathcal{T} \tag{34}$$

The fourth term in (30) are the total expenditures of DEG operation, which comprises degradation and fuel costs. The latter, can be calculated as a quadratic function of the power delivered [53]. Therefore, the total costs associated to DEG operation are given by:

$$f^{\mathrm{DEG}} = \sum_{\forall t \in \mathcal{T}} \left\{ \Delta\tau \cdot \left[ u_t^{\mathrm{DEG}} \cdot \left( \frac{\kappa^{\mathrm{DEG}} \cdot \overline{p}^{\mathrm{DEG}}}{T^{\mathrm{DEG}}} + \omega_1^{\mathrm{DEG}} \right) + p_t^{\mathrm{DEG}} \cdot \omega_2^{\mathrm{DEG}} + \left( p_t^{\mathrm{DEG}} \right)^2 \cdot \omega_3^{\mathrm{DEG}} \right] \right\} \quad (35)$$

In this paper, the quadratic term in (35) is linearized by using efficient piecewise representation (see Appendix B). The remainder terms in (30) account for the operational and maintenance costs of renewable generators and the hydrogen-based storage system. For renewable units, these costs are proportional to the total energy generated, as said the equation (36) [48]:

$$f^{i} = \sum_{\forall t \in \mathcal{T}} \left\{ \Delta\tau \cdot p_t^{i} \cdot \mu^{i} \right\};\ \forall i \in \{\mathrm{PV}, \mathrm{WG}\} \quad (36)$$

While in the case of the HSS, along the maintenance expenditures, the startup and shutdown costs and equipment degradation have to be included, as follows [54]:

$$f^{i} = \sum_{\forall t \in \mathcal{T}} \left\{ \Delta\tau \cdot \left( \frac{\kappa^{i} \cdot \overline{p}^{i}}{T^{i}} \cdot u_t^{i} + p_t^{i} \cdot \mu^{i} \right) + \nu^{i} \cdot \left( \mathrm{on}_t^{i} + \mathrm{off}_t^{i} \right) \right\};\ \forall i \in \{\mathrm{EZ}, \mathrm{FC}\} \quad (37)$$

## 4 - Solution Procedure

This section describes the procedure for robust solution of the optimal scheduling tool developed in Section 3, using interval notation of uncertain parameters. The proposed optimization problem is performed into three stages. The first one corresponds to the conventional deterministic scheduling model, in which the uncertain parameters take their expected values. As a result of this stage, the scheduling plan for the different assets and sheddable consumers is passed to the second step, in which the most favorable/unfavorable values of the forecast variables are calculated. To this end, the uncertainties are taken as decision variables, allowing them to vary within the predicted intervals. In this stage, the effect of the uncertainties in the objective function (30) is evaluated. Thus, it is assumed that an uncertain parameter takes favorable values if it supposes a reduction of the operational cost, while the unfavorable values increment the monetary expenditures. Finally, the third stage receives the information of the second stage and adjusts the scheduling plan accordingly. To this end, the deterministic model is again solved in this stage, but taking the value of uncertainties calculated at stage 2 (favorable or unfavorable values depending of the strategy taken). The proposed procedure allows to adjust the degree in which the predicted intervals are considered, which indirectly set the level of uncertainty assumed by the operator. This is modelled by introducing the so-called uncertain level $\xi$, whose importance is later highlighted.

Inspired by [39], an iterative procedure is proposed to robust scheduling of the MG under study. The proposed algorithm is illustrated in the flowchart of Fig. 5. By this procedure, firstly the deterministic solution is calculated taking the expected value of uncertainties. After, the value of the uncertainties and the scheduling plan are progressively updated each iteration, by iteratively running the stages 2 and 3. Each stage updates the deterministic and uncertainties solution, and passes this information to the following stage. The process is finalized when the solution of both stages no longer vary, which is determined by the following stopping criterion:

$$\frac{\left|f_k^{(2)}-f_k^{(3)}\right|}{f_k^{(2)}} \leq tol \qquad (38)$$

where the subscript denotes the $k^{th}$ iteration of the iterative procedure; $f^{(2)}$ and $f^{(3)}$ are the values of the objective function (3) in the stages 2 and 3, respectively; and $tol$ is a preset convergence threshold which is fixed equal to 0.01 in this work. It is worth noting that the scheduling plan can be executed under optimistic or pessimistic perspectives depending on the impact of uncertainties in the objective function. In the former case, the uncertainties are assumed to impact negatively on the objective function, while in the latter, the uncertainties take favorable values. Therefore, the optimistic strategy finds the value of uncertainties that minimizes the objective function (30), while the pessimistic perspective finds those values of uncertainties that maximize the monetary expenditures. In this regard, the optimistic and pessimistic perspectives can be conceived as the risk-seeker and risk-averse strategies in [55], respectively.

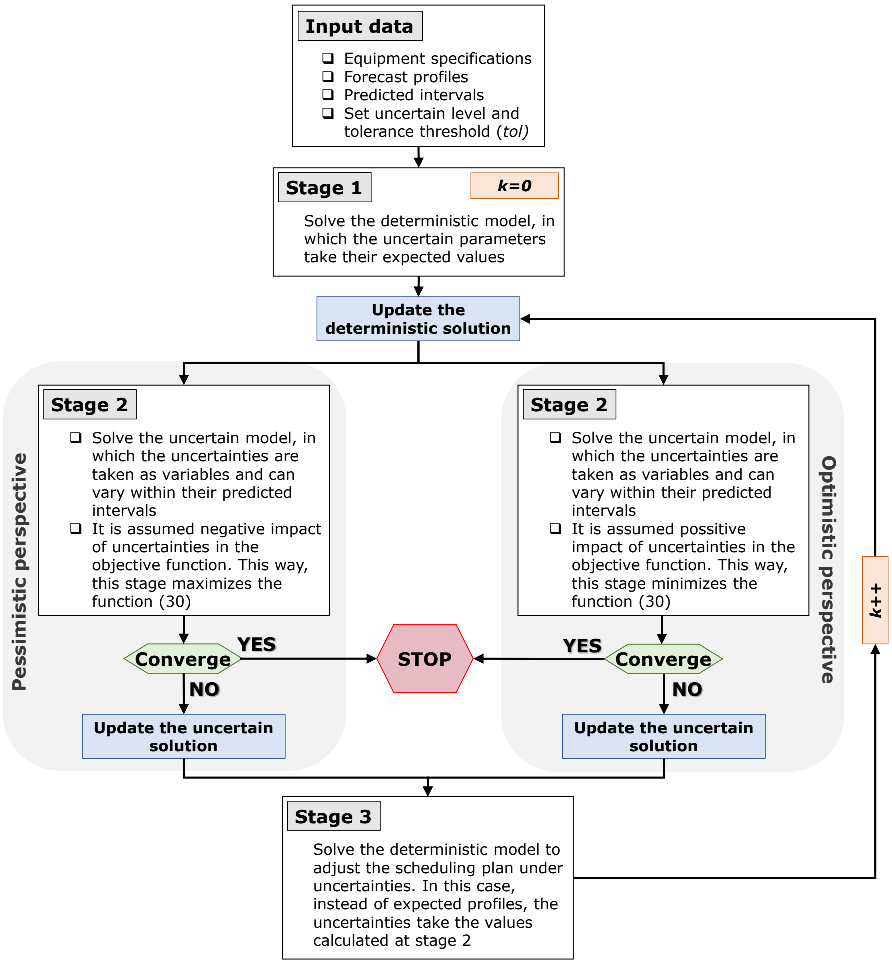


Figure 5 - Flowchart of the developed procedure for robust optimal scheduling of the MG under study

As commented, the stage 1 of the developed algorithm determines the scheduling plan from a deterministic point of view, which can be calculated by running the following optimization problem:

$$\boldsymbol{u}^{\text{det}} \rightarrow \arg\min_{\boldsymbol{w},\boldsymbol{u}} f(\mathbb{E}[\boldsymbol{\Omega}]) \tag{39}$$

Subject to (11)-(37)

As seen, the problem (39) seeks to minimize the operational cost assuming expected profiles of the uncertain parameters, while conventional control signals such as commitment status and power set-points are the variables of the problem.

The second stage receives information calculated in the first step, and determines the most favorable/unfavorable values of the uncertain parameters. This way, the stage 2 takes the uncertain parameters as variables, which are modelled as interval numbers following the notation described in Section 3.1. In this case, limits of each uncertain variable are determined by the predicted intervals and the introduced uncertain level, as expressed in (40).

$$\mathbb{E}[a_t] - \xi \cdot [a_t]^{\downarrow} \leq [a_t] \leq \mathbb{E}[a_t] + \xi \cdot [a_t]^{\uparrow};\ \forall t \in \mathcal{T} \wedge a \in \mathbf{\Omega} \tag{40}$$

As seen in (40), the uncertain level determines the degree in which the predicted intervals are considered in the optimization problem. Thus, if $\xi = 1$, the entire interval is considered. In this case, the operator assumes a high degree of uncertainty. Otherwise, the problem becomes deterministic if $\xi = 0$. The most typical solution consists on fixing $\xi \in (0,1)$, which supposes that a certain degree of uncertainty is assumed.

The stage 2 can be solved under pessimistic or optimistic perspectives. In the former case, it is assumed that uncertain variables have a negative impact on the objective function, which is mathematically represented by the following optimization problem:

$$\mathbf{\Omega}^{\mathrm{unc}} \rightarrow \arg\max_{\boldsymbol{w}} f\left(\boldsymbol{u}^{\mathrm{det}}, [\mathbf{\Omega}]\right) \tag{41a}$$

Subject to (11)-(37), (40)

Indeed, the most unfavourable value of the uncertain parameters is attained when the objective function is maximized, as said the problem (41a). At this stage, the commitment plan calculated at stage 1 is assumed fixed, being only possible to control some continuous signals like power set-points of shiftable consumers. In this manner, the pessimistic uncertain conditions are calculated for a given commitment plan. In contrast, if the MG is operated under an optimistic point of view, the uncertain variables positively impacts on the objective function, thus minimizing the operational cost as said the problem (41b).

$$\boldsymbol{\Omega}^{\mathrm{unc}} \rightarrow \arg\min_{\boldsymbol{w}} f\left(\boldsymbol{u}^{\mathrm{det}}, [\boldsymbol{\Omega}]\right) \tag{41b}$$

Subject to (11)-(37), (40)

Finally, the stage 3 seeks the scheduling plan which minimizes the operational cost under favorable/unfavorable uncertain profiles. In this way, this stage adjusts the scheduling plan according to the value of uncertainties calculated in the stage 2, which is stated in the following optimization problem:

$$\boldsymbol{u}^{\mathrm{det}} \rightarrow \arg\min_{\boldsymbol{w},\boldsymbol{u}} f(\boldsymbol{\Omega}^{\mathrm{unc}}) \tag{42}$$

## 5 - Case study

This section presents a case study to validate the developed Mixed-Integer-Linear-Logical programming model for scheduling of isolated MGs, and the iterative solution procedure for robust optimization. To this purpose, the benchmark MG depicted in Fig. 1 has been considered, for which the mathematical model developed in Section 3 is used. The developed optimization model is coded in Matlab R2019a and is solved using Gurobi [56]. All the simulations are performed using an Intel® CoreTM i5-9400F, 2.90 GHz, 8.00 GB RAM, personal computer.

In order to compare the computational burden of the developed methodology with other similar approaches, the optimization model described in Section 3 was run for a variety of scenarios under stochastic programming. To this end, the methodology described in [49] was used to create (and posteriorly reduced to a set of representative profiles) the scenario-space for the uncertain parameters. Although the results obtained with both methodologies cannot be directly compared since stochastic programming does not look for extreme values of uncertainties, a comparison of the computational times give an idea about the computational performance of both techniques. In this sense, the developed procedure took approximately 3-5 minutes to be completed, which improved by 15-25% the performance of the stochastic approach. These results are due to under stochastic programming all the variables are bi-dimensional (no. of scenarios × time horizon), resulting in a very high computational cost. In addition, the observed runtimes are considered acceptable for scheduling tools, which are performed over day-ahead time horizons.

### *5.1 - Input data*

The scheduling plan of the MG is performed over a 24 hours horizon with 30 minutes time resolution. Fig. 6 plots the weather and demand forecasts with their associated predicted interval. The weather information is extracted from [57], and correspond with the values observed at Virgin Islands (U.S.) on May 3, 2016; whereas the demand profile is built scaling down the consumption at La Palma Island (Spain) on May 3, 2016 [58]. Three sheddable consumers are considered whose forecast demand and predicted intervals are plotted in Fig. 7. Penalty costs for these consumers are established in 550, 700 and 900 $/h for each consumer, respectively. The cost of non-served load is fixed at 100 $/kWh in order to avoid unserved energy, while the data of shiftable consumers are collected in Table 2. Lastly, Tables 3-8 report the parameters of DEG, PV array, WG units, EZ, FC and HSS, respectively.

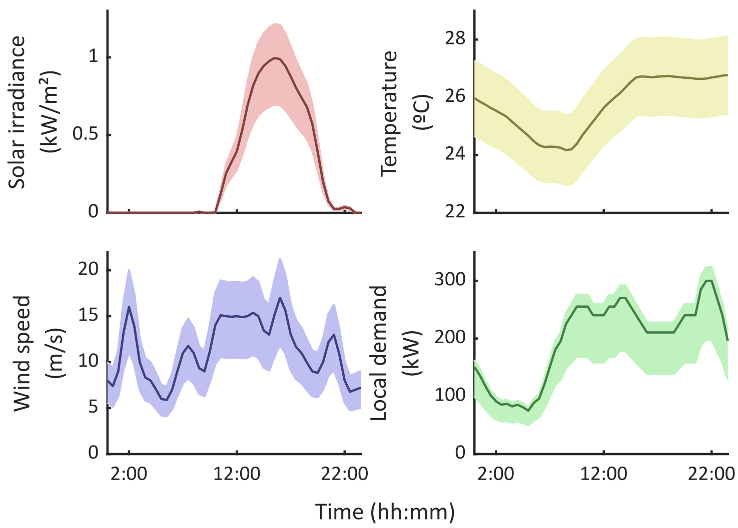


Figure 6 - Forecast profiles and predicted intervals of uncertain parameters

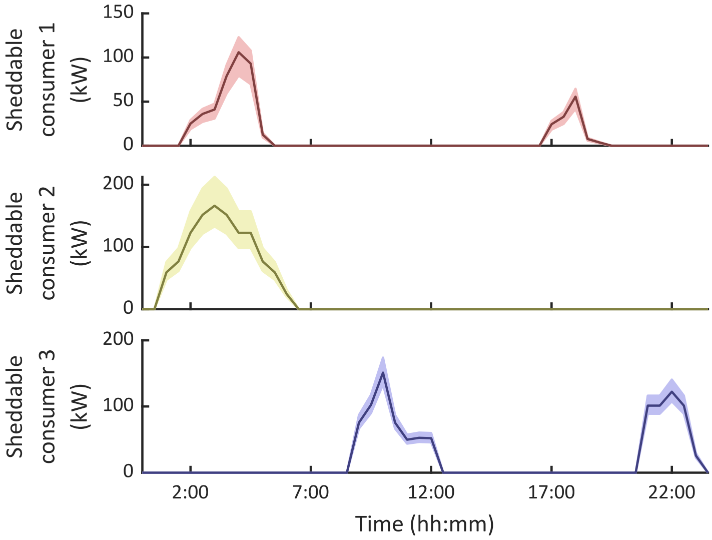


Figure 7 - Expected demand of sheddable consumers and associated confidence intervals

Table 2 - Data of shiftable consumers

| **Parameter** | **Consumer 1** | **Consumer 2** |
|---|---|---|
| $\varepsilon$ (kWh) | 900 | 700 |
| $\overline{p}$ (kW) | 100 | 100 |
| $\upsilon$ (\$/kWh) | 6.10 | 6.10 |

Table 3 - Data of DEG [49, 53]

| **Parameter** | **Value** |
|---|---|
| $\overline{p}, \underline{p}$ (kW) | 750, 50 |
| $RU$, $RD$ (kW) | 200, 200 |
| $T$ (h) | 30,000 |
| $\kappa$ (\$/kW) | 340 |
| $\omega_1, \omega_2, \omega_3$ (\$/h, \$/kWh, \$/kWh$^2$) | 0.6, 0.05, 0.02 |

Table 4 - Data of PV units [48]

| **Parameter** | **Value** |
|---|---|
| $\overline{p}$ (kW) | 350 |
| $\eta$ | 0.167 |
| $\mu$ (\$/kWh) | 0.14 |

Table 5 - Data of WG units [48]

| **Parameter** | **Value** |
|---|---|
| $\overline{p}$ (kW) | 300 |
| $\underline{\gamma}, \gamma^*, \overline{\gamma}$ (m/s) | 2, 11, 21 |
| $\alpha, \beta$ kW·(m/s)$^{-3}$, - | 0.2268, 0.006 |
| $\eta$ | 0.88 |
| $\mu$ (\$/kWh) | 0.19 |

Table 6 - Data of EZ [54, 59]

| **Parameter** | **Value** |
|---|---|
| $\overline{p}$, $\underline{p}$ (kW) | 400, 25 |
| $RU$, $RD$ (kW) | 300, 300 |
| $\eta$ | 0.65 |
| $T$ (h) | 10,000 |
| $\kappa$ (\$/kW) | 8.50 |
| $\nu$ (\$) | 0.15 |
| $\mu$ (\$/kWh) | 0.03 |

Table 7 - Data of HSS [19]

| **Parameter** | **Value** |
|---|---|
| $\overline{v}$ ($m^3$) | 25 |
| $\overline{g}$, $\underline{g}$ (bar) | 13.8, 2 |
| $\theta$ (K) | 313 |

Table 8 - Data of FC [53, 59]

| **Parameter** | **Value** |
|---|---|
| $\overline{p}$, $\underline{p}$ (kW) | 400, 25 |
| $RU$, $RD$ (kW) | 300, 300 |
| $\eta$ | 0.77 |
| $T$ (h) | 10,000 |
| $\kappa$ (\$/kW) | 32 |
| $\nu$ (\$) | 0.02 |
| $\mu$ (\$/kWh) | 0.03 |

### *5.2 - Results*

Fig. 8 plots the value of the objective function for different uncertain levels. As seen, the operation cost decreases when the uncertain level grows under a pessimistic point of view, while the opposite trend is observed under an optimistic strategy. This result is logic since under a pessimistic perspective it is assumed that the uncertain parameters have a negative impact on the objective function. Hence, if the uncertain level grows, it is expected that the operation cost grows as well, while the contrary behavior can be equally deduced under an optimistic point of view.

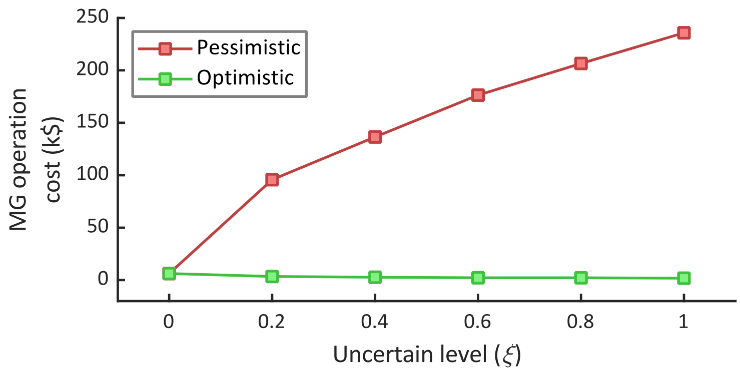


Figure 8 - Total MG operation cost for different uncertain levels

Similar behavior can be deduced for other variables. For example, let us focus on the behavior of flexible demand. Fig. 9 shows the total hours that sheddable consumers were necessarily disconnected from the system, as seen, this result grows with the uncertain level under a pessimistic strategy while the opposite trend is observed under an optimistic point of view. The same conclusions can be extracted for the shiftable demands, as observed in Fig. 10 where the total non-served energy (%) is plotted for different uncertain levels. In this case, energy requirements of these users are expected to be totally satisfied in the deterministic case and under an optimistic strategy, however, unserved energy may grow by ~90% under a pessimistic point of view.

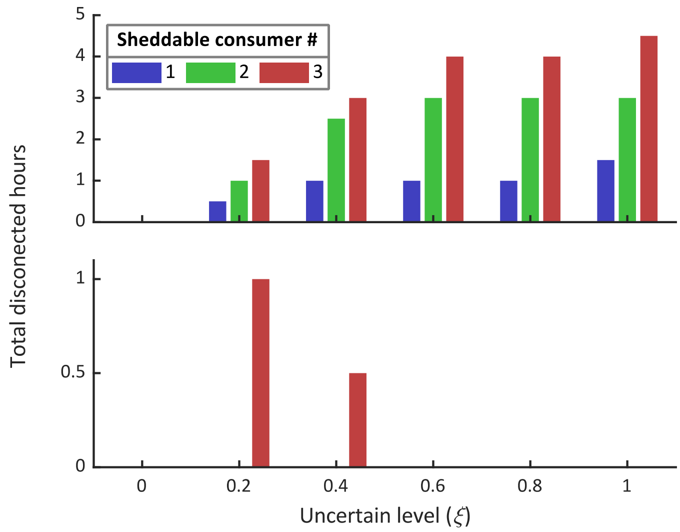


Figure 9 - Total disconnected hours of sheddable consumers for different uncertain levels under pessimistic (top) and optimistic (bottom) strategies

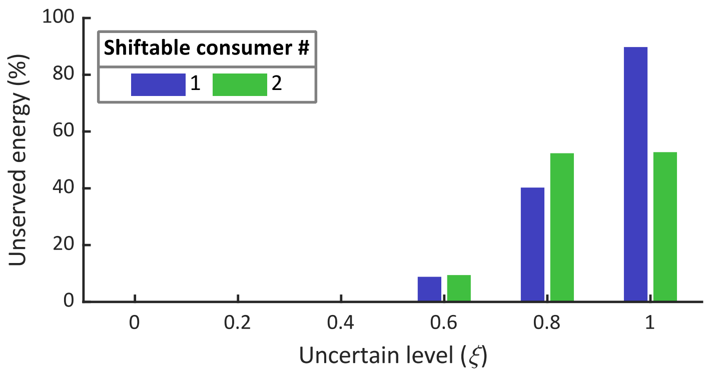


Figure 10 - Total unserved energy hours of shiftable consumers for different uncertain levels under a pessimistic strategy (100% of energy was covered in the optimistic case for all the range of uncertain levels)

Now, the behavior of the green hydrogen-based storage system is analyzed. Fig. 11 shows the total energy absorbed/produced by EZ/FC. As seen, the exploitation of the storage facility decreases with the uncertain level under a pessimistic perspective, while the opposite behavior is observed with optimistic strategies. The responsible of these results is the surplus renewable energy. As observed in Fig. 12 where total surplus renewable energy is plotted for various uncertain levels, the excess of renewable generation drastically decreases with the degree of uncertainty under a pessimistic point of view, which hinders the exploitation of the storage facility. This last aspect is better appreciated in Fig. 13, where the state of pressure of the HSS is plotted for different uncertain levels under pessimistic strategy. It can be noted that the storage facility is progressively less exploited as the uncertain level grows.

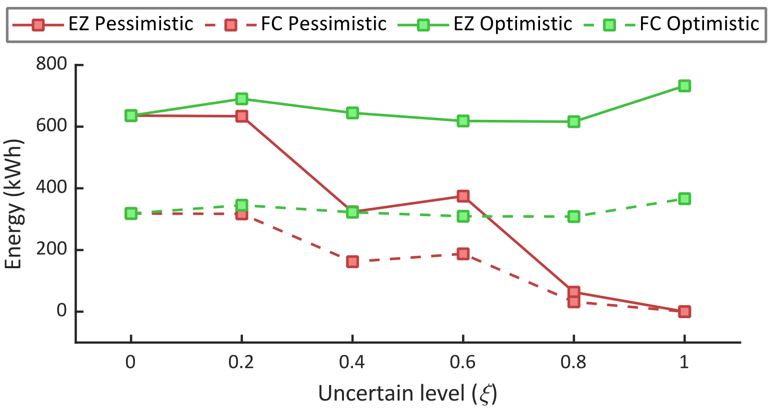


Figure 11 - Total energy absorbed/produced by EZ/FC for different uncertain levels

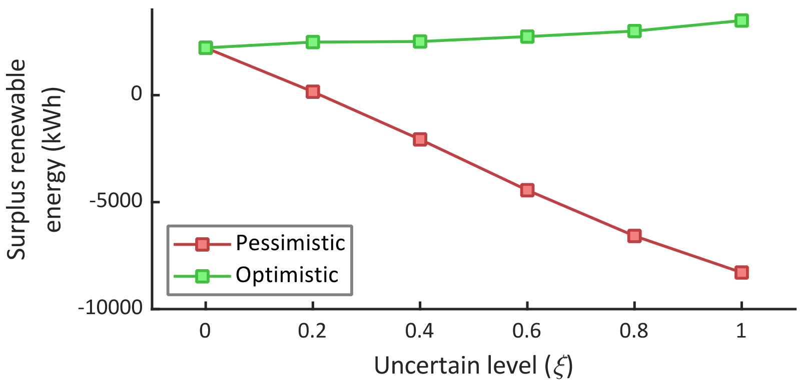


Figure 12 - Total surplus renewable energy for different uncertain levels

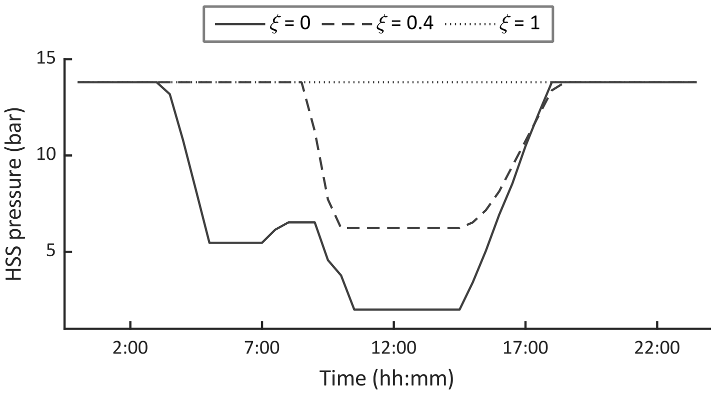


Figure 13 - State of pressure of the HSS for different uncertain levels under a pessimistic perspective

Finally, we analyze how the uncertain level affects the dependency of fossil fuels (i.e. backup generation. Fig. 14 analyses this aspect showing the total working hours and energy generated by the DEG for different uncertain levels. As expected, dependency of the backup generation grows with the uncertain level if a pessimistic strategy is assumed, while the opposite trend is manifested under an optimistic perspective. Nevertheless, total disconnection of DEG is not possible any case, due to negative surplus renewable energy has to be inevitably covered by the backup generator.

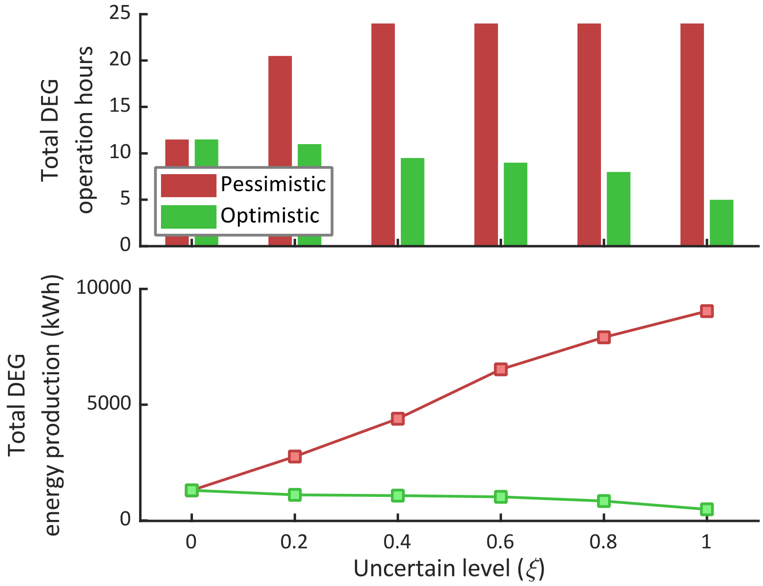


Figure 14 - Total DEG operation hours and energy production for different uncertain levels

## 6 - Conclusions

This paper has presented a novel optimal scheduling model for isolated MGs, encompassing a green hydrogen-based storage system and demand response programs. In the developed tool, green hydrogen generation is modelled by logical rules, which are incorporated into the Mixed-Integer-Linear programming optimization model using Mixed-Integer-Logical formulation. Since the green hydrogen production is explicitly modelled, it is ensured that totally of the hydrogen generated is green, which may result vital to address certain governmental initiatives. Uncertainties in renewable generation and local demand are handled by an original interval formulation and iterative solution procedure. The proposal allows to perform the scheduling plan from pessimistic and optimistic perspectives, being therefore adaptable to different operational strategies adopted by the operator.

Extensive simulations have been performed on a benchmark MG model. Preliminary experiments revealed that the developed optimization model is fully competitive with other standard approaches like stochastic programming. In fact, substantial computational savings were observed, thus validating the developed tool for day-ahead scheduling applications. Numerical experiments allowed to analyze how the different scheduling strategies (pessimistic or optimistic) impact on different operating aspects. For example, it has been observed a decreasing exploitation of the hydrogen storage facility for increasing uncertain levels in pessimistic environments, while the dependency of backup generation and total operation cost increases. The degree of uncertainty also affects consumers subjected to DR programs, which are generally less covered as the uncertain grows. In general, the opposite trend was observed in the different results when the system is operated under an optimistic point of view. This way, the results revealed the effectiveness of the new proposal to handle with uncertainties in hydrogen-based MGs, highlighting its practical implications in industry tools. The developed model is modular enough to be easily applied to other systems. In addition, its particular versatile structure allows to incorporate real-time control modules, thus providing a totally usefulness tools for MG operators.

In the future, we will study the applicability of the new proposal in multi-energy hubs, home energy management tools and electric vehicle recharging stations.

## Appendix A - Linearization of products of continuous and integer variables

Let us consider k integer variables $\delta_i, \forall i \in \{1,2,\dots,k\}$ and a continuous variable $x$, then the product of the integer variables by the continuous one can be replaced by the linear dummy variable $z = x \cdot \delta_1 \cdot \delta_2 \cdot \dots \cdot \delta_k$ by imposing the constraints (A1) and (A2) [49].

$$x - \sum_{i=1}^{i=k}\{M \cdot (1-\delta_i)\} \le z \le x + \sum_{i=1}^{i=k}\{M \cdot (1-\delta_i)\} \quad \text{(A1)}$$

$$-M \cdot \delta_i \le z \le M \cdot \delta_i;\ \forall i \in \{1,2,\dots,k\} \quad \text{(A2)}$$

## Appendix B - Linearization of quadratic and cubic terms

To linearize quadratic and cubic terms, we use an efficient piecewise representation of the nonlinear function (e.g. see [52]). Let us denote the nonlinear function $\psi$ of which its limits are known. Then, the range of the concerned function is divided into $n$ points, so that its piecewise representation is given by:

$$\tilde{\psi} = \langle \tilde{x}_i, \psi(\tilde{x}_i) \rangle; \forall i \in \{1,2,\dots,n\} \tag{B1}$$

Wherever the nonlinear term appears in the problem, it can be replaced by the dummy variable $z$, which is calculated as:

$$z = \sum_{i=2}^{i=n} \{\delta_i \cdot (K_i \cdot x + L_i)\} \tag{B2}$$

where $\delta$ is a binary SOS1 [51], and $K$, $L$ are respectively calculated, as follows:

$$K_i = \frac{\psi(\tilde{x}_i) - \psi(\tilde{x}_{i-1})}{\tilde{x}_i - \tilde{x}_{i-1}};\ \forall i \in \{2,3,\dots,n\} \tag{B3}$$
$$L_i = \psi(\tilde{x}_i) - K_i \cdot \tilde{x}_i;\ \forall i \in \{2,3,\dots,n\} \tag{B4}$$

By declaring $\delta$ as a SOS1, one ensures that only one segment of (B1) is activated at once. Finally, the constraint in (B5) links $\delta$ with the set of points $\tilde{x}$.

$$\sum_{i=1}^{i=n-1} \{\delta_i \cdot \tilde{x}_i\} \leq x \leq \sum_{i=2}^{i=n} \{\delta_{i-1} \cdot \tilde{x}_i\} \tag{B5}$$

The products of integer and continuous variables that appear in (B1) can be linearized following the strategy described in Appendix A.

**Appendix C - Linearization of bi-linear terms**

To linearize bi-linear terms, we use one of the advanced piecewise representations developed in [51]. More precisely, we use the formulation denoted as 'nf4l' in this reference, because its good trade-off between computational burden and accuracy. Let us consider the product of the continuous variables $x$ and $y$, which will be replaced in the model by the dummy variable $z$. Let use declare the integer set $\delta$ as a SOS1 and the grid-point partitioning of the domain of $x$, as follows:

$$x \approx \langle \tilde{x}_i \rangle; \forall i \in \{0,1,\dots,n\} \tag{C1}$$

Thereby, the variable $x$ is approximated by its piecewise representation, which is constructed by introducing the continuous variable $\Delta\tilde{x}$ and the constraints (C2)-(C4):

$$m_i = \tilde{x}_i - \tilde{x}_{i-1}; \forall i \in \{0,1,\dots,n\} \tag{C2}$$
$$x = \sum_{i=1}^{i=n} \{\delta_i \cdot \tilde{x}_{i-1} + \Delta\tilde{x}_i\} \tag{C3}$$
$$0 \leq \Delta\tilde{x}_i \leq m_i \cdot \delta_i;\ \forall i \in \{0,1,\dots,n\} \tag{C4}$$

Similarly, the variable $y$ can be represented by the limits of its domain and the continuous variable $\Delta y$, which represents the deviation of the continuous variable from its lower bound. This model is implemented with the constraints (C5) and (C6).

$$y = \underline{y} + \sum_{i=1}^{i=n}\{\Delta y_i\} \tag{C5}$$

$$0 \leq \Delta y_i \leq \left(\overline{y} - \underline{y}\right) \cdot \delta_i;\ \forall i \in \{0,1,\dots,n\} \tag{C6}$$

Finally, the variable $z$ can be effectively calculated with (C7) by linking the representations of the variables $x$ and $y$ above, for which, the continuous variable $\Delta z$ has to be declared, whose bounds are given in (C8)-(C10).

$$z = \underline{y} \cdot x + \sum_{i=1}^{i=n}\{\tilde{x}_{i-1} \cdot \Delta y_i\} + \Delta z \tag{C7}$$

$$\Delta z \geq \sum_{i=1}^{i=n}\{m_i \cdot \Delta y_i\} + \left(\overline{y} - \underline{y}\right) \cdot \sum_{i=1}^{i=n}\{\Delta \tilde{x}_i - m_i \cdot \delta_i\} \tag{C8}$$

$$\Delta z \leq \left(\overline{y} - \underline{y}\right) \cdot \sum_{i=1}^{i=n}\{\Delta \tilde{x}_i\} \tag{C9}$$

$$\Delta z \leq \sum_{i=1}^{i=n}\{m_i \cdot \delta_i\} \tag{C10}$$

## References


[1] IRENA. *Hydrogen: A Renewable Energy Perspective*. Tokyo, Japan, 2019. Online available at: https://www.irena.org/publications/2019/Sep/Hydrogen-A-renewable-energy-perspective, (accessed Jun. 29, 2021).

[2] G. Kakoulaki, I. Kougias, N. Taylor, F. Dolci, J. Moya, A. Jäger-Waldau. Green hydrogen in Europe - A regional assessment: Substituting existing production with electrolysis powered by renewables. *Energy Conversion & Management* 2021; 228: 113649. https://doi.org/10.1016/j.enconman.2020.113649.

[3] European Commission. *The European Green Deal*. Brussels, Belgium: COM(2019) 640 final, 2019. Online available at: https://ec.europa.eu/info/sites/default/files/european-green-deal-communication_en.pdf, (accessed Jun. 29, 2021).

[4] European Commission. *Horizon Europe - The next EU Research & Innovation Investment Programme (2021-2027)*. 2019. Online available at: https://ec.europa.eu/info/sites/default/files/research_and_innovation/strategy_on_research_and_innovation/presentations/horizon_europe_en_investing_to_shape_our_future.pdf, (accessed Jun. 29, 2021).

[5] European Commission. *A hydrogen strategy for a climate-neutral Europe*. vol. 53. Brussels, Belgium; 2020. https://doi.org/10.1017/CBO9781107415324.004.

[6] H. Ito, N. Miyazaki, M. Ishida, A. Nakano. Efficiency of unitized reversible fuel cell systems. *International Journal of Hydrogen Energy* 2016; 41(13): 5803-15. https://doi.org/10.1016/j.ijhydene.2016.01.150.

[7] Y. Li, T. V. Nguyen. Core-shell rhodium sulfide catalyst for hydrogen evolution reaction / hydrogen oxidation reaction in hydrogen-bromine reversible fuel cell. *Journal of Power Sources* 2018; 382: 152-9. https://doi.org/10.1016/j.jpowsour.2018.02.005.

[8] V.-T. Giap, Y. S. Kim, Y. D. Lee, K. Y. Ahn. Waste heat utilization in reversible solid oxide fuel cell systems for electrical energy storage: Fuel recirculation design and feasibility analysis. *Journal of Energy Storage* 2020; 29: 101434. https://doi.org/10.1016/j.est.2020.101434.

[9] M. Lo Faro, et al. The role of CuSn alloy in the co-electrolysis of $CO_2$ and $H_2O$ through an intermediate temperature solid oxide electrolyser. *Journal of Energy Storage* 2020; 27: 100820. https://doi.org/10.1016/j.est.2019.100820.
[10] C. Tarhan, M. A. Çil. A study on hydrogen, the clean energy of the future: Hydrogen storage methods. *Journal of Energy Storage* 2021; 40: 102676. https://doi.org/10.1016/j.est.2021.102676.
[11] D. Zhu, Y. Ait-Amirat, A. N'Diaye, A. Djerdir. On-line state of charge estimation of embedded metal hydride hydrogen storage tank based on state classification. *Journal of Energy Storage* 2021; 42: 102950. https://doi.org/10.1016/j.est.2021.102950.
[12] M. Marinelli, M. Santarelli. Hydrogen storage alloys for stationary applications. *Journal of Energy Storage* 2020; 32: 101864. https://doi.org/10.1016/j.est.2020.101864.
[13] M. Vahid-Ghavidel, M. S. Javadi, M. Gough, S. F. Santos, M. Shafie-Khah, J. P. S. Catalão. Demand Response Programs in Multi-Energy Systems: A Review. *Energies* 2020; 13(17): 4332. https://doi.org/10.3390/en13174332.
[14] B. Zakeri, S. Syri. Electrical energy storage systems: A comparative life cycle cost analysis. *Renewable & Sustainable Energy Reviews* 2015; 42: 569-96. https://doi.org/10.1016/j.rser.2014.10.011.
[15] M. Faisal, M. A. Hannan, P. J. Ker, A. Hussain, M. B. Mansor, F. Blaabjerg. Review of Energy Storage System Technologies in Microgrid Applications: Issues and Challenges. *IEEE Access* 2018; 6: 35143-64. https://doi.org/10.1109/ACCESS.2018.2841407.
[16] S. Nojavan, K. Zare, B. Mohammadi-Ivatloo. Application of fuel cell and electrolyzer as hydrogen energy storage system in energy management of electricity energy retailer in the presence of the renewable energy sources and plug-in electric vehicles. *Energy Conversion & Management* 2017; 136: 404-17. https://doi.org/10.1016/j.enconman.2017.01.017.
[17] S. Nojavan, K. Zare, B. Mohammadi-Ivatloo. Selling price determination by electricity retailer in the smart grid under demand side management in the presence of the electrolyser and fuel cell as hydrogen storage system. *International Journal of Hydrogen Energy* 2017; 42(5): 3294-308. https://doi.org/10.1016/j.ijhydene.2016.10.070.
[18] J. Liu, C. Chen, Z. Liu, K. Jermsittiparsert. N. Ghadimi. An IGDT-based risk-involved optimal bidding strategy for hydrogen storage-based intelligent parking lot of electric vehicles. *Journal of Energy Storage* 2020; 27: 101057. https://doi.org/10.1016/j.est.2019.101057.
[19] J. Jannati, D. Nazarpour. Optimal energy management of the smart parking lot under demand response program in the presence of the electrolyser and fuel cell as hydrogen storage system. *Energy Conversion & Management* 2017; 138: 659-69. https://doi.org/10.1016/j.enconman.2017.02.030.
[20] J. Jannati, D. Nazarpour. Multi-objective scheduling of electric vehicles intelligent parking lot in the presence of hydrogen storage system under peak load management. *Energy* 2018; 163: 338-50. https://doi.org/10.1016/j.energy.2018.08.098.
[21] A. F. Marzoghi, S. Bahramara, F. Adabi, S. Nojavan. Optimal scheduling of intelligent parking lot using interval optimization method in the presence of the electrolyser and fuel cell as hydrogen storage system. *International Journal of Hydrogen Energy* 2019; 44(45): 24997-5009. https://doi.org/10.1016/j.ijhydene.2019.07.226.
[22] A. F. Marzoghi, S. Bahramara, F. Adabi, S. Nojavan. Interval multi-objective optimization of hydrogen storage based intelligent parking lot of electric vehicles under peak demand management. *Journal of Energy Storage* 2020; 27: 101123. https://doi.org/10.1016/j.est.2019.101123.
[23] W. Wang, et al. Performance Evaluation of a Hydrogen-Based Clean Energy Hub with Electrolyzers as a Self-Regulating Demand Response Management Mechanism. *Energies* 2017; 10(8): 1211. https://doi.org/10.3390/en10081211.
[24] M. A. Mirzaei, A. S. Yazdankhah, B. Mohammadi-Ivatloo. Integration of Demand Response and Hydrogen Storage System in Security Constrained Unit Commitment with High Penetration of Wind Energy. In *Iranian Conference on Electrical Engineering (ICEE)* 2018; Mashhad, Iran: 1203-8. https://doi.org/10.1109/ICEE.2018.8472631.

[25] F. Kholardi, M. Assili, M. A. Lasemi, A. Hajizadeh. Optimal Management of Energy Hub with Considering Hydrogen Network. In *2018 International Conference on Smart Energy Systems and Technologies (SEST)* 2018; Seville, Spain: 1-6. https://doi.org/10.1109/SEST.2018.8495664.

[26] M. Ali, J. Ekström, M. Lehtonen. Sizing Hydrogen Energy Storage in Consideration of Demand Response in Highly Renewable Generation Power Systems. *Energies* 2018; 11(5): 1113. https://doi.org/10.3390/en11051113.

[27] J. Naughton, P. Mancarella, M. Cantoni. Demand Response from an Integrated Electricity-Hydrogen Virtual Power Plant. In *2019 IEEE International Conference on Environment and Electrical Engineering and 2019 IEEE Industrial and Commercial Power Systems Europe (EEEIC / I&CPS Europe)* 2019; Genova, Italy: 1-6. https://doi.org/10.1109/EEEIC.2019.8783329.

[28] N. A. El-Taweel, H. Khani, H. E. Z. Farag. Hydrogen Storage Optimal Scheduling for Fuel Supply and Capacity-Based Demand Response Program Under Dynamic Hydrogen Pricing. *IEEE Transactions on Smart Grid* 2019; 10(4): 4531-42. https://doi.org/10.1109/TSG.2018.2863247.

[29] S. Seyyedeh-Barhagh, M. Majidi, S. Nojavan, K. Zare. Optimal Scheduling of Hydrogen Storage under Economic and Environmental Priorities in the Presence of Renewable Units and Demand Response. *Sustainable Cities & Society* 2019; 46: 101406. https://doi.org/10.1016/j.scs.2018.12.034.

[30] D. Yu, J. Wang, D. Li, K. Jermsittiparsert, S. Nojavan. Risk-averse stochastic operation of a power system integrated with hydrogen storage system and wind generation in the presence of demand response program. *International Journal of Hydrogen Energy* 2019; 44(59): 31204-215. https://doi.org/10.1016/j.ijhydene.2019.09.222.

[31] M. A. Mirzaei, A. S. Yazdankhah, B. Mohammadi-Ivatloo. Stochastic security-constrained operation of wind and hydrogen energy storage systems integrated with price-based demand response. *International Journal of Hydrogen Energy* 2019; 44(27): 14217-27. https://doi.org/10.1016/j.ijhydene.2018.12.054.

[32] A. Mansour-Saatloo, M. A. Mirzaei, B. Mohammadi-Ivatloo, K. Zare. A Risk-Averse Hybrid Approach for Optimal Participation of Power-to-Hydrogen Technology-Based Multi-Energy Microgrid in Multi-Energy Markets. *Sustainable Cities & Society* 2020; 63: 102421. https://doi.org/10.1016/j.scs.2020.102421.

[33] M. N. Heris, et al. Evaluation of hydrogen storage technology in risk-constrained stochastic scheduling of multi-carrier energy systems considering power, gas and heating network constraints. *International Journal of Hydrogen Energy* 2020; 45(55): 30129-41. https://doi.org/10.1016/j.ijhydene.2020.08.090.

[34] M. J. Shabani, S. M. Moghaddas-Tafreshi. Fully-decentralized coordination for simultaneous hydrogen, power, and heat interaction in a multi-carrier-energy system considering private ownership. *Electric Power Systems Research* 2020; 180: 106099. https://doi.org/10.1016/j.epsr.2019.106099.

[35] M. R. Maghami, R. Hassani, C. Gomes, H. Hizam, M. L. Othman, M. Behmanesh. Hybrid energy management with respect to a hydrogen energy system and demand response. *International Journal of Hydrogen Energy* 2020; 42(3): 1499-509. https://doi.org/10.1016/j.ijhydene.2019.10.223.

[36] A. Mansour-Saatloo, M. Agabalaye-Rahvar, M. A. Mirzaei, B. Mohammadi-Ivatloo, M. Abapour, K. Zare. Robust scheduling of hydrogen based smart micro energy hub with integrated demand response. *Journal of Cleaner Production* 2020; 267: 122041. https://doi.org/10.1016/j.jclepro.2020.122041.

[37] A. Mansour-Saatloo, et al. A hybrid robust-stochastic approach for optimal scheduling of interconnected hydrogen-based energy hubs. *IET Smart Grid* 2021; 4(2): 241-54. https://doi.org/10.1049/stg2.12035.

[38] I. AlHajri, A. Ahmadian, A. Elkamel. Stochastic day-ahead unit commitment scheduling of integrated electricity and gas networks with hydrogen energy storage (HES), plug-in electric vehicles (PEVs) and renewable energies. *Sustainable Cities & Society* 2021; 67: 102736. https://doi.org/10.1016/j.scs.2021.102736.

[39] B. Wang, C. Zhang, Z. Y. Dong. Interval Optimization Based Coordination of Demand Response and Battery Energy Storage System Considering SOC Management in a Microgrid. *IEEE Transactions on Sustainable Energy* 2020; 11(4): 2922-31. https://doi.org/10.1109/TSTE.2020.2982205.

[40] N.G. Paterakis, O. Erdinç, A.G. Bakirtzis, J.P.S. Catalão. Optimal Household Appliances Scheduling Under Day-Ahead Pricing and Load-Shaping Demand Response Strategies. *IEEE Transactions on Industrial Informatics* 2015; 11(6): 1509-19. https://doi.org/10.1109/TII.2015.2438534.

[41] J. Ren, S. R. Gamble, A. J. Roscoe, J. T. S. Irvine, G. Burt. Modeling a Reversible Solid Oxide Fuel Cell as a Storage Device Within AC Power Networks. *Fuel Cells* 2012; 12(5): 773-86. https://doi.org/10.1002/fuce.201100185.

[42] F. Sayed, S. Kamel, M. Tostado-Véliz, F. Jurado. Congestion Management in Power System Based on Optimal Load Shedding Using Grey Wolf Optimizer. In *IEEE Middle East Power Systems Conference (MEPCON 2018)* 2018; Cairo, Egypt. https://doi.org/10.1109/MEPCON.2018.8635208.

[43] R. J. Hyndman. *Forecasting: Principles and Practice*, 3rd ed. Melbourne, Australia: OTexts, 2019.

[44] S. Zeinal-Kheiri, A. M. Shotorbani, A. Khardenavis, B. Mohammadi-Ivatloo, R. Sadiq, K. Hewage. An adaptive real-time energy management system for a renewable energy-based microgrid. *IET Renewable Power Generation* 2021. https://doi.org/10.1049/rpg2.12223.

[45] V. Hosseinnezhad, M. Shafie-Khah, P. Siano, J. P. S. Catalão. An Optimal Home Energy Management Paradigm With an Adaptive Neuro-Fuzzy Regulation. *IEEE Access* 2020; 8: 19614-28. https://doi.org/10.1109/ACCESS.2020.2968038.

[46] R. E. Moore, *Methods and applications of interval analysis*. Philadelphia, PA, USA: SIAM, 1979.

[47] X. Kou, F. Li. Interval Optimization for Available Transfer Capability Evaluation Considering Wind Power Uncertainty. *IEEE Transactions on Sustainable Energy* 2020; 11(1): 250-9. https://doi.org/10.1109/TSTE.2018.2890125.

[48] P. Arévalo, M. Tostado-Véliz, F. Jurado. A novel methodology for comprehensive planning of battery storage systems. *Journal of Energy Storage* 2021; 37: 102456. https://doi.org/10.1016/j.est.2021.102456.

[49] M. Tostado-Véliz, R. S. León-Japa, F. Jurado. Optimal electrification of off-grid smart homes considering flexible demand and vehicle-to-home capabilities. *Applied Energy* 2021; 298: 117184. https://doi.org/10.1016/j.apenergy.2021.117184.

[50] M. Tostado-Véliz, M. Bayat, A. A. Ghadimi, F. Jurado. Home Energy Management in off-grid Dwellings: Exploiting Flexibility of Thermostatically Controlled Appliances. *Journal of Cleaner Production* 2021; 310: 127507. https://doi.org/10.1016/j.jclepro.2021.127507.

[51] C. E. Gounaris, R. Misener, C. A. Floudas. Computational Comparison of Piecewise-Linear Relaxations for Pooling Problems. *Industrial & Engineering Chemistry Research* 2009; 48(12): 5742-66. https://doi.org/10.1021/ie8016048.

[52] M. Tostado-Véliz, P. Arévalo, F. Jurado. A comprehensive electrical-gas-hydrogen Microgrid model for energy management applications. *Energy Conversion & Management* 2020; 228: 113726. https://doi.org/10.1016/j.enconman.2020.113726.

[53] L. Alvarado-Barrios, A. R. del Nozal, J. B. Valerino, I. G. Vera, J. L. Martínez-Ramos. Stochastic unit commitment in microgrids: Influence of the load forecasting error and the availability of energy storage. *Renewable Energy* 2020; 146: 2060-9. https://doi.org/10.1016/j.renene.2019.08.032.

[54] F. Garcia-Torres, D. G. Vilaplana, C. Bordons, P. Roncero-Sánchez, M. A. Ridao. Optimal Management of Microgrids With External Agents Including Battery/Fuel Cell

Electric Vehicles. *IEEE Transactions on Smart Grid* 2019; 10(4): 4299-308. https://doi.org/10.1109/TSG.2018.2856524.

[55] M. Daneshvar, B. Mohammadi-Ivatloo, K. Zare, S. Asadi, A. Anvari-Moghaddam. A Novel Operational Model for Interconnected Microgrids Participation in Transactive Energy Market: A Hybrid IGDT/Stochastic Approach. *IEEE Transactions on Industrial Informatics* 2021; 17(6): 4025-35. https://doi.org/10.1109/TII.2020.3012446.

[56] Gurobi - The fastest solver. https://www.gurobi.com/, (accessed June 28, 2021).

[57] National Centers for Environmental Information. Land-Based Datasets and Products. Online available at: https://www.ncdc.noaa.gov/data-access/land-based-station-data/land-based-datasets, (accessed June 28, 2021).

[58] Red Eléctrica de España. Canary electricity demand in real-time. Online available at: https://www.ree.es/en/activities/canary-islands-electricity-system/canary-electricity-demand-in-real-time, (accessed June 28, 2021).

[59] Y. Jiang, L. Guo. Research on Wind Power Accommodation for an Electricity-Heat-Gas Integrated Microgrid System With Power-to-Gas. *IEEE Access* 2019; 7: 87118-26. https://doi.org/10.1109/ACCESS.2019.2924577.